

# USING GENERALISED SUPPLY-DEMAND ANALYSIS TO IDENTIFY REGULATORY METABOLITES

**JOHANN M. ROHWER<sup>1,\*</sup> AND JAN-HENDRIK S. HOFMEYR<sup>1,2</sup>**

<sup>1</sup>Triple-J Group for Molecular Cell Physiology, Department of Biochemistry, and

<sup>2</sup>Centre for Studies in Complexity, Stellenbosch University, Private Bag X1,  
ZA-7602 Matieland, South Africa

E-Mail: \*[jr@sun.ac.za](mailto:jr@sun.ac.za)

*Received: 22<sup>nd</sup> February 2010 / Published: 14<sup>th</sup> September 2010*

## ABSTRACT

We present the framework of generalised supply-demand analysis of a kinetic model of a cellular system, which can be applied to networks of arbitrary complexity. By fixing the concentrations of each of the variable species in turn and varying them in a parameter scan, rate characteristics of supply-demand are constructed around each of these species. The shapes of the rate characteristic patterns and the magnitude of the flux-response coefficients of the supply and demand blocks, as compared to the elasticities of the enzymes that interact directly with the fixed metabolite, allow for identification of regulatory metabolites in the system. The analysis provides information not only on whether and where the system is functionally differentiated, but also on the degree to which of its species are homeostatically buffered. The novelty in our method lies in the fact it is unbiased, supplying an entry point for the further analysis and detailed characterisation of large models of cellular systems, in which the choice of metabolite around which to perform a supply-demand analysis is not always obvious. The method is exemplified with two kinetic models from the published scientific literature.

## I INTRODUCTION

The burgeoning field of systems biology (*e.g.* [1]) has developed out of the realisation that biological systems cannot be understood from reductionist characterisation of their components alone, but that their interactions have to be integrated in a “systems” framework. New models of diverse cellular pathways appear regularly and are curated and stored in online databases [2, 3]; such models provide powerful tools that are often more accessible to query and interrogation than experimental systems. Yet without proper frameworks of analysis, these models, albeit big and comprehensive, remain little more than collections of data.

The framework of supply-demand analysis (SDA), developed by Hofmeyr and Cornish-Bowden [4], has proved useful in studying the regulation of cellular pathways within the metaphor of an economy controlled by supply and demand. It has become a reference framework for analysing metabolic pathways by teaching scientists to look for flux control beyond the scope of what has traditionally been called the pathway, *i.e.* in the demand for its end-product, a view that has subsequently been corroborated by experimental data (*e.g.* [5]). While SDA can provide useful results, its application to large kinetic models of cellular pathways is, however, hampered by the problem that their complexity may preclude us from finding a “natural” subdivision of the system into supply and demand blocks. With this in mind, we have generalised SDA so that it can be applied to models of arbitrary size and complexity in a systematic, computer-driven way [6].

In the remainder of this paper we first summarise generalised supply-demand analysis as developed in [6] (Section 2), and subsequently apply it to two published kinetic models (Section 3).

## 2 PRINCIPLES AND ILLUSTRATION OF GENERALISED SUPPLY-DEMAND ANALYSIS

Ordinary supply-demand analysis (SDA) [4] considers the subdivision of a pathway around a central intermediate, with the block or blocks of reactions contributing to the production of the intermediate constituting the “supply”, and those that contribute to its consumption, the “demand”. The behaviour of the system around the steady-state point is assessed with a so-called combined rate characteristic [7], which depicts how the rates of supply and demand vary with changes in the concentration of the intermediate. The intersection of the supply and demand rate characteristics signifies the steady-state point. If the rate characteristic is drawn in double-logarithmic space, the elasticities [8] of supply and demand towards the intermediate can be read off directly as slopes of the tangents to the supply and demand curves at the steady-state point, enabling the calculation of control coefficients. One of the main tenets of SDA is that when one of the two blocks controls the flux, the other one determines the degree of homeostasis in the intermediate; such a system has been termed *functionally differentiated* [4].

---

*In silico* SDA with a kinetic model can be easily achieved by making the intermediate around which the rate characteristic is to be constructed, into a fixed (clamped) species of the model, thus turning it into a model parameter. This parameter is then varied over a wide range through a parameter scan. An implicit assumption of this approach is that the system has been or can readily be partitioned into supply and demand; however, when faced with the complexity of cellular pathways or of large models of such pathways, the choice of intermediate around which to perform the SDA is often far from obvious.

To address this shortcoming, we have generalised SDA in such a way that it can easily be performed on a kinetic models of any cellular system, large or small, without requiring prior knowledge of its regulatory structure [6]. Generalised supply-demand analysis (GSDA) works in the following way: *Each* of the variable intermediates is *clamped in turn* and thus made into a parameter of the system. Its concentration is then varied above and below the reference steady-state value in the original system through a parameter scan, and the fluxes through the supply and demand reactions that are directly connected to the intermediate are plotted on a log-log rate characteristic. Every flux that directly produces the intermediate is a separate supply flux, and likewise, each flux that directly consumes it is a separate demand flux. There will thus be as many rate characteristics as there are reactions that produce or consume the intermediate. It should be emphasised that this procedure is valid for arbitrary models and does not presuppose a subdivision of the system into supply and demand blocks.

GSDA yields as many combined rate characteristic graphs as there are variable species in the system. As will be shown below, the following important features about the regulation of the system can be identified from the shapes of the curves and associated elasticities and response coefficients:

1. Potential sites of regulation;
2. Regulatory metabolites;
3. The quantitative relative contribution of different routes of interaction from an intermediate to a supply or demand block;
4. Sites of functional differentiation where one of the supply or demand blocks predominantly controls the flux, and the other determines the degree of homeostatic buffering of the intermediate.

We next exemplify GSDA with a model of a linear 5-enzyme pathway containing a feedback loop.

---

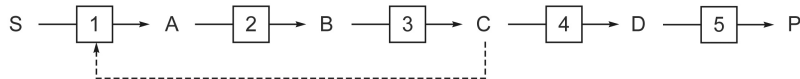


**Figure 1.** A five-enzyme linear pathway converting substrate S to product P. In one of the models, the first enzyme is allosterically inhibited by intermediate C (see main text). Reproduced with permission from [6].

### 2.1 GSDA of a Simple Linear Pathway

The simulations in this section use two variants of a kinetic model of the linear pathway in Figure 1 (detailed model descriptions and computational methods are provided in [6]).

**Model I** This is the base-line, undifferentiated version in which all five enzymes have identical kinetic parameters and are modelled with reversible Michaelis-Menten kinetics (with the exception of enzyme 5, which is modelled with irreversible Michaelis-Menten kinetics). There is no allosteric feedback from C to enzyme 1.

**Model II** In this model, enzyme 1 is inhibited allosterically by C and is modelled with reversible Hill kinetics [9]. The limiting rates of enzymes 2 and 3 have been increased so that they are close to equilibrium. Enzymes 4 and 5 together have almost complete control over the flux through the pathway.

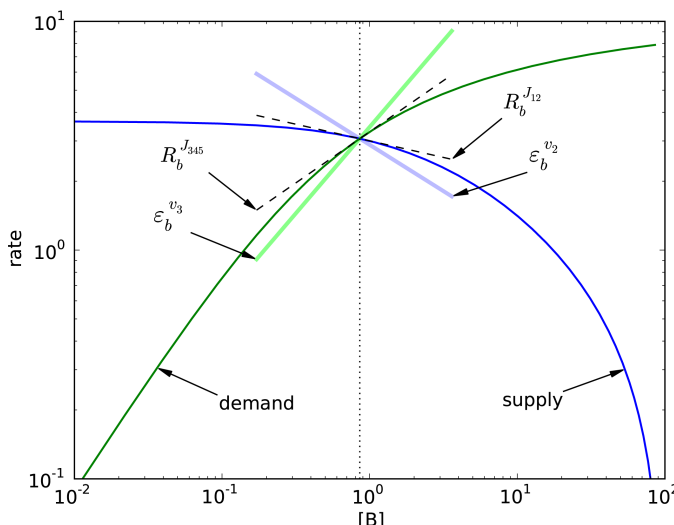


**Figure 2.** Supply-demand analysis around metabolite B for Model I. The concentration of B was clamped and varied to generate the supply and demand rate characteristics, as described in the text. The steady-state concentration is indicated by a vertical dotted line. The rate characteristics, response coefficients (tangents to the rate characteristics at the steady-state point) and elasticities of the supply and demand enzymes directly connected to B are labelled on the graph. Reproduced with permission from [6].

As explained above, a GSDA is performed by clamping each variable species of the model in turn and varying its concentration to generate the supply and demand rate characteristics. This yields graphs such as in Figure 2, which shows the GSDA around metabolite B in model I. To facilitate the interpretation of such graphs, this specific case is discussed in detail. The intersection of the log-log rate characteristics of supply and demand marks the steady-state point. The supply rate characteristic is drawn in blue and the demand rate characteristic in green. The slopes of the tangents to the rate characteristics (indicated by dashed lines on the graph) equal the flux-response coefficients (see *e.g.* [8]) of supply and demand towards B (in Figure 2,  $J_{12}$  signifies the flux through the supply block and  $J_{345}$  that through the demand block). These response coefficients quantify how sensitively the supply and demand fluxes respond towards changes in  $b$ , and are equivalent to “block-elasticities” [10] or co-response coefficients [11, 12] in the complete system where B is not clamped.

SDA as originally described [4] assumes that the only communication between supply and demand is via the linking intermediate. In this situation, the supply-demand block control coefficients of the complete pathway can be directly calculated from the supply and demand block elasticities, and the distribution of flux control is determined by the ratio of the block elasticities, while the magnitude of concentration control is determined by the difference  $\varepsilon_b^{v_{345}} - \varepsilon_b^{v_{12}}$ . Figure 2 also shows graphically the elasticities of the enzymes that produce or consume B. Elasticities are local properties of enzymes and quantify how sensitively an enzyme’s local rate responds to changes in a substrate, product or effector. They are in fact apparent kinetic orders. In this case B is a product of  $v_2$  and a substrate for  $v_3$ , so Figure 2 shows  $\varepsilon_b^{v_2}$  (thick light blue line) and  $\varepsilon_b^{v_3}$  (thick light green line).

The crux of GSDA now lies in the comparison of the values of the response coefficients with the elasticities of the enzymes that are directly connected to the clamped metabolite. In Figure 2, these values differ, *i.e.*  $R_b^{J_{12}} \neq \varepsilon_b^{v_2}$  and  $R_b^{J_{345}} \neq \varepsilon_b^{v_3}$ . In other cases, they will be seen to agree. However, before comparing them in detail, first we have to present the GSDA of all metabolites for both models.

The graphs in Figure 3 present the results of the GSDA on models I and II. To avoid clutter, the graphs are not annotated but they follow the same convention as Figure 2. The only additional piece of information required is that of an allosteric modifier elasticity ( $\varepsilon_c^{v_1}$  in Fig. 3b with C clamped, as only model II has the feedback loop). This is drawn in an orange line to set it apart from the supply and demand elasticities.

---

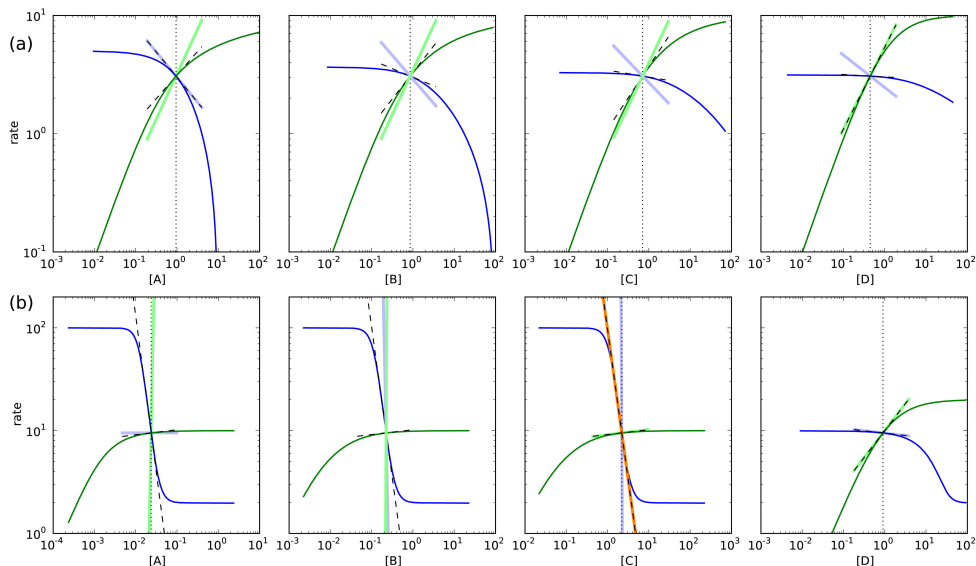


**Figure 3.** Generalised supply-demand analysis of the system depicted in Fig. 1. The concentrations of A–D were clamped in turn and varied to generate the supply and demand rate characteristics, as described in the text. The supply rate characteristic is drawn in blue, that for the demand in green. The steady-state concentration of the clamped metabolite is indicated by a vertical dotted line. The response coefficients of the supply and demand blocks are indicated by black dashed lines. The elasticities of the supply and demand enzymes for the clamped intermediate they are directly connected to are indicated by thick lines of the same colour as the rate characteristic. Model variants: (a) model I, (b) model II (see main text). In (b), the allosteric elasticity  $\varepsilon_c^{v_1}$  is indicated by an orange thick line. Adapted from [6] with permission.

## 2.2 Interpretation of Generalised Supply-demand Analysis Graphs

The graphs in Figure 3 contain a wealth of information. As shown in [6], they can be interpreted on four levels, i.e. differences in the rate characteristic shapes as one proceeds from one metabolite to the next in the pathway, comparison of elasticity and response slopes, identification of points of functional differentiation and homeostasis, and finally, refined analysis through partial response coefficients.

### DIFFERENCES IN RATE CHARACTERISTIC SHAPES

The first assessment criterion of GSDA merely looks at the general shapes of the supply and demand rate characteristics and is not yet concerned with elasticities and response coefficients. In model I (Fig. 3a) all enzymes have identical kinetics and the overall shapes of the rate characteristics are similar for metabolites A–D. In model II (Fig. 3b), however, the pattern for D is different from those for A–C (which are still similar). This means that the kinetic properties of enzyme 4 are such that site of regulation has been introduced into the

system. In this specific case the reason is that enzyme 4 has been made insensitive to changes in the concentration of C ( $\varepsilon_c^{v_4} \approx 0$ ). In general, such zero elasticities, whether towards substrate or product, induce a change in the rate characteristic shape because they shift the flux control to demand or supply, respectively. Overall, changes in the rate characteristic shapes thus pin-point potential sites of regulation.

## COMPARISON OF ELASTICITIES AND RESPONSE COEFFICIENTS

GSDA can be extended to a second level by comparing the values of the elasticities and flux-response coefficients at the steady-state point for each metabolite. From the partitioned response property of control analysis [8],

$$R_p^J = \varepsilon_p^{v_i} \times C_{v_i}^J \quad (1)$$

it follows that  $R_p^J = \varepsilon_p^{v_i}$  if  $C_{v_i}^J = 1$ . This means that the enzyme on which the intermediate acts directly must have full control over its own flux. Figure 3 shows that in general response and elasticity coefficients differ. There are, however, a few notable exceptions. The first of these is the trivial case of the first and last metabolites in the chain (A and D): Response coefficients and elasticities will generally agree because the supply block for A and demand block for D each consist only of a single enzyme. (The exception of  $\varepsilon_a^{v_1} \neq R_a^{J_1}$  in Figure 3b has to do with the feedback loop and is further discussed in [6]).

Aside from the trivial case, any agreement between elasticity and response coefficient points to a site of regulation. Equation 1 shows that the response coefficient can equal the elasticity either if the control coefficient is one (as discussed above), or if the elasticity is zero (which effectively makes the value of the control coefficient irrelevant). The first case obtains, for example, in Figure 3b with C clamped, where  $\varepsilon_c^{v_1} = R_c^{J_{123}}$  (feedback loop with  $C_{v_1}^{J_{123}} = 1$ ). Here, C can be classified as a “regulatory metabolite” with respect to its supply block because the flux response of this supply towards the clamped metabolite concentration is exactly the same as the activity response (i.e. elasticity) of the enzyme directly affected by the clamped metabolite. The flux-control coefficient of one causes the flux response to be transmitted fully through the block.

The second case (zero elasticity) obtains, for example, in Figure 3b, where  $\varepsilon_c^{v_4} = R_c^{J_{45}} \approx 0$ . Such a zero elasticity confers flux control (in the complete system) to that particular block and results in functional differentiation of the system, which is further discussed below.

## FUNCTIONAL DIFFERENTIATION AND HOMEOSTASIS

SDA has shown that when one block (say, demand) controls the flux through a pathway, the other (say, supply) will determine the degree of control of the intermediate [4]. Such a pathway has been termed “functionally differentiated” as flux and concentration control

---

are functions of different blocks. Complete flux control by a supply or demand block (over the whole pathway) can easily be identified by a zero response coefficient (i.e. block elasticity) of that block towards the intermediate (e.g.  $R_c^{J_{45}}$  in Fig. 3b). The response coefficient of the other block ( $R_c^{J_{123}}$ ) will then determine the degree of homeostasis in the intermediate: the larger its numerical value, the better the homeostatic buffering.

Model II (Fig. 3b) has been discussed in detail as an example of a functionally differentiated system in the context of SDA [4, 13], and the arguments will not be repeated here. Suffice it to say that the properties of the feedback elasticity  $\varepsilon_c^{v_1}$ , which equals  $R_c^{J_{123}}$  here, set the steady-state concentration of C and determine its degree of homeostatic buffering. In this sense, the steady-state concentration of C can be regarded as “regulated”. Why C can be considered a “regulatory” metabolite when considering the supply block in isolation has been discussed above.

## MULTIPLE ROUTES OF INTERACTION

When two or more direct routes of interaction exist from a clamped metabolite to a particular supply or demand block, GSDA can be further refined by dissecting the response coefficient into partial response coefficients. An example is the GSDA around metabolite C in Figure 1, where C can affect both enzymes 1 and 3 directly (the former through allosteric inhibition, the latter through product inhibition). By calculating the total response coefficient as the sum of the two partial response coefficients referring to each of these routes of interaction, their individual contribution to the total response coefficient can be quantified and depicted graphically. This will not be further discussed here, and the reader is referred to [6].

## 3 REAL MODELS

The linear pathway in Figure 1 can be regarded as quite artificial, although it illustrates some important regulatory features observed in metabolic pathways. To demonstrate the wider applicability of our approach, we now perform a GSDA on two kinetic models of real pathways from the literature.

### 3.1 Threonine Biosynthesis in *Escherichia coli*

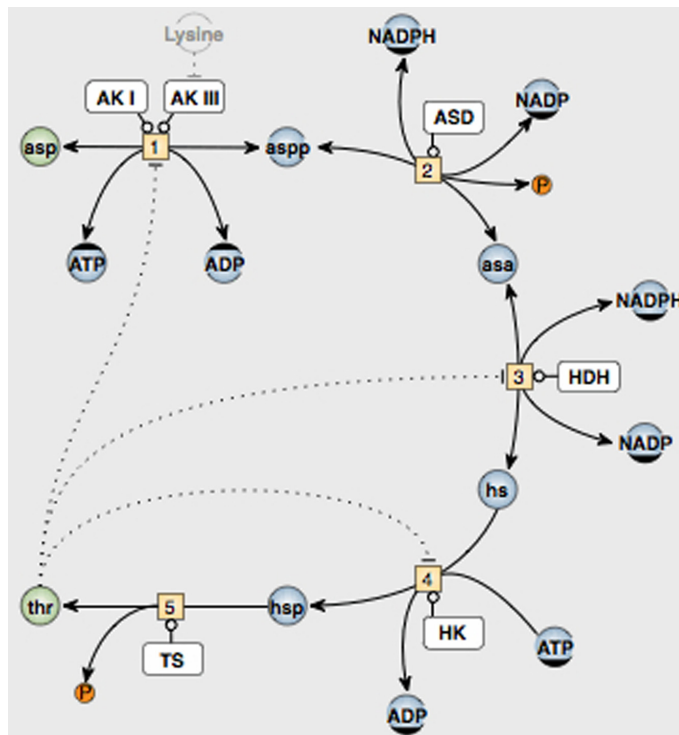


**Figure 4.** Pathway of threonine biosynthesis in *Escherichia coli* as modelled in [14]. Abbreviations: *asp*, aspartate; *aspp*,  $\beta$ -aspartyl phosphate; *asa*, aspartate  $\beta$ -semialdehyde; *hs*, homoserine; *hsp*,  $O$ -phospho-homoserine; *thr*, threonine; *AK*, aspartate kinase; *ASD*, aspartate semialdehyde dehydrogenase; *HDH*, homoserine dehydrogenase; *HK*, homoserine kinase; *TS*, threonine synthase. Image reproduced from JWS Online (<http://jjj.biochem.sun.ac.za>) with permission.

The first model is of the threonine biosynthesis pathway in *Escherichia coli*, and was developed by Chassagnole *et al.* in 2001 [14] (the pathway structure is given in Fig. 4).

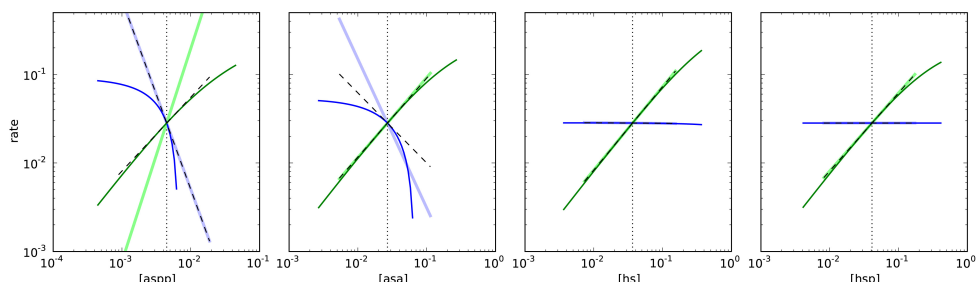


**Figure 5.** GSDA of the threonine biosynthesis model of [14]. Abbreviations are defined in Fig. 4.

As was done for the model of the linear pathway in Figure 1, each of the intermediates (aspp, asa, hs and hsp) was now in turn made into a parameter of the model and scanned around its reference steady-state value. The results are shown in Figure 5 using the same conventions as previously. Homoserine and phospho-homoserine act as regulatory metabolites in the sense that the flux-response coefficients of their respective supply and demand blocks equal the elasticities of the enzymes directly connected to them. Aspartate-semialdehyde has a similar effect on its demand (homoserine dehydrogenase), but is not regulatory with respect to its supply enzyme, aspartate semialdehyde dehydrogenase-response and elasticity coefficients differ. Aspartyl-phosphate is not a regulatory metabolite (the fact that the elasticity and response coefficients agree for aspartate kinase has to do with the fact that this is the first enzyme in the pathway and the “supply” of aspartyl phosphate only consists of a single enzyme; see Section 2.2 above).

The results can be understood and interpreted as follows. In the model [14] the first two steps (aspartate kinase and aspartate semialdehyde dehydrogenase) are close to equilibrium, leading to large elasticity values for aspartyl phosphate and aspartate semialdehyde. Consequently, elasticities and response coefficients do not agree. Homoserine kinase and threonine synthase (the last two steps) are modelled as irreversible reactions [14], resulting in zero product elasticities. The insensitivity to their products allows these enzymes to transmit any changes in their substrate concentrations downstream, hence the response coefficients and elasticities for these substrates agree (Fig. 5, panels 3 and 4). Homoserine dehydrogenase seems to follow a similar pattern: its substrate elasticity and flux-response coefficient towards aspartate semialdehyde are equal (Fig. 4, panel 2), while its product elasticity is zero (Fig. 4, panel 3). Although the enzyme is modelled with reversible kinetics, the large value of the equilibrium constant (3162, [14]) makes it behave like an effectively irreversible reaction.

### **3.2 Erythrocyte Glycolysis**

The second example concerns a kinetic model of the free-energy and redox metabolism of erythrocytes [15]. For lack of space, we do not show the complete GSDA, but rather focus on the branch-point at glucose-6-phosphate. This metabolite is produced in the hexokinase (HK) reaction, and can then be further metabolised by phosphoglucoisomerase (PGI) in the Embden-Meyerhof-Parnas pathway, or by glucose-6-phosphate dehydrogenase (G6PDH) in the pentose phosphate pathway.

---

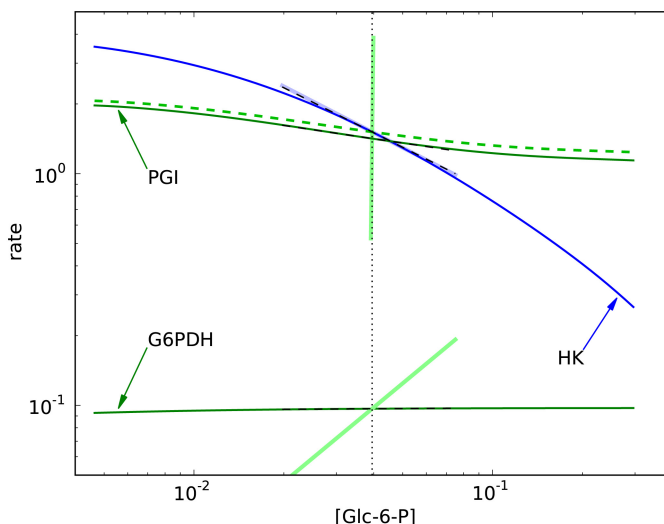


**Figure 6.** GSDA around the metabolite glucose-6-phosphate in the kinetic model of erythrocyte metabolism of Holzhütter [15]. The graph follows the same convention as previously. For description and discussion see text. Abbreviations: *Glc-6-P*, glucose-6-phosphate; *HK*, hexokinase; *PGI*, phosphoglucoisomerase; *G6PDH*, glucose-6-phosphate dehydrogenase.

The results of the GSDA, performed by clamping the glucose-6-phosphate concentration in the model, varying it around its steady-state value and monitoring the supply (HK) and demand (PGI and G6PDH) fluxes, is shown in Figure 6. This graph differs from Figures 2, 3 and 5 in that it describes a branch-point with two demand fluxes. As discussed in detail in [6], such a case is treated by plotting the sum of the demand fluxes as a green dotted line. The steady state can be read off from the graph where this line intersects the single (blue) supply rate characteristic. The flux-response coefficients and elasticities are plotted for each demand flux separately; in this way the regulatory function of glucose-6-phosphate can be separately assessed for the two branches.

Figure 6 shows that glucose-6-phosphate acts as a regulatory metabolite with respect to its supply (i.e. the elasticity and response coefficient are the same). This is a non-trivial case, since the supply in this model consists of two reactions (glucose transport and HK). However, it can be understood quite readily because glucose transport is modelled as facilitated diffusion and is close to equilibrium in the reference steady state calculated by the model. In contrast to the supply, glucose-6-phosphate is not a regulatory metabolite for either of the demand fluxes (the response and elasticity coefficients differ for both PGI and G6PDH).

Another result from Figure 6, which may appear paradoxical at first, is that the response coefficient of the PGI flux towards glucose-6-phosphate is negative (i.e. increasing glucose-6-phosphate concentrations cause this flux to decrease), although it is a demand flux.

The elasticity of PGI is positive as expected, and moreover has a very large value since the enzyme is close to equilibrium. The reason for the negative response coefficient is that the response of lower glycolysis to glucose-6-phosphate is not only mediated via its effect on PGI, but also through the levels of the ATP/ADP and NAD<sup>+</sup>/NADH moieties, which are treated as variables in the model.

#### **4 CONCLUDING REMARKS**

This paper has described generalised supply-demand analysis as a method for identifying and characterising regulatory metabolites in kinetic models of cellular pathways. The method can be generally applied to complex networks. The approach involves clamping each of the variable species of the model in turn and varying their concentration over a range in a parameter scan. The rate characteristics of supply and demand of that particular species are then generated and plotted, together with straight lines representing the elasticities of the enzymes directly connected to the clamped intermediate, and the response coefficients of the supply and demand blocks. GSDA can pinpoint potential sites of regulation in a pathway, identify regulatory metabolites and sites of functional differentiation, and quantify the importance of different routes of interaction in a pathway [6].

In addition, to our knowledge the results presented in Figures 5 and 6 are the first application of GSDA to kinetic models of “real” pathways and exemplify how the analysis can be used to identify regulatory metabolites from such models.

As discussed in detail in [6], there are obvious inter-relations between GSDA and the “modular” [16] or “top-down” [17, 18] approaches to control analysis, and if there are no additional routes of communication between the supply and demand blocks other than through the intermediate, all enzymes belonging to a particular block (say, supply) form a “monofunctional unit” [19]. GSDA, however, goes further than these “classical” approaches to control analysis: first, by considering the behaviour of the system over a wide range, a broader picture of its control and regulation (*e.g.* in the face of varying demand loads) is obtained than from a mere set of control and elasticity coefficients at a single steady-state point; and second, the rate characteristics and associated elasticity slopes provide a visual picture that allows easy inference of which block controls the flux, to what extent the intermediate is homeostatically buffered, etc.

In conclusion, the strength of GSDA lies in the fact that it provides a computational tool for the systematic functional analysis of large “silicon-cell”-type kinetic models. The tool has been implemented in the ratechar module of the PySCeS software [20], which has been developed in our group. This provides an easy-to-use general interface that allows the user to perform a GSDA on a model with minimal additional programming. Moreover, since PySCeS can import SBML files [21], models can be imported from public databases such as JWS Online [2] or BioModels [3] and do not need to be re-coded. By including all model

species in the analysis, human bias is removed and regulatory metabolites can be readily identified. In subsequent refined analyses, the modeller can then focus on and zoom in on those parts of the model exhibiting interesting regulatory behaviour.

## ACKNOWLEDGEMENTS

This work was supported by the National Research Foundation and the National Bioinformatics Network (South Africa).

## REFERENCES

- [1] Kitano, H. (2002) Computational systems biology. *Nature* **420**:206 – 210.  
doi: <http://dx.doi.org/10.1038/nature01254>.
  - [2] Olivier, B.G. and Snoep, J.L. (2004) Web-based kinetic modelling using JWS Online. *Bioinformatics* **20**:2143 – 2144.  
doi: <http://dx.doi.org/10.1093/bioinformatics/bth200>.
  - [3] LeNovère, N., Bornstein, B., Broicher, A., Courtot, M., Donizelli, M., Dharuri, H., Li, L., Sauro, H., Schilstra, M., Shapiro, B., Snoep, J.L. and Hucka, M. (2006) BioModels Database: a free, centralized database of curated, published, quantitative kinetic models of biochemical and cellular systems. *Nucleic Acids Res.* **34**:D689 – D691.  
doi: <http://dx.doi.org/10.1093/nar/gkj092>.
  - [4] Hofmeyr, J.-H.S. and Cornish-Bowden, A. (2000) Regulating the cellular economy of supply and demand. *FEBS Lett.* **476**:47 – 51.  
doi: [http://dx.doi.org/10.1016/S0014-5793\(00\)01668-9](http://dx.doi.org/10.1016/S0014-5793(00)01668-9).
  - [5] Koebmann, B.J., Westerhoff, H.V., Snoep, J.L., Nilsson, D. and Jensen, P.R. (2002) The glycolytic flux in *Escherichia coli* is controlled by the demand for ATP. *J. Bacteriol.* **184**:3909 – 3916.  
doi: <http://dx.doi.org/10.1128/JB.184.14.3909-3916.2002>.
  - [6] Rohwer, J.M. and Hofmeyr, J.-H.S. (2008) Identifying and characterising regulatory metabolites with generalised supply-demand analysis. *J. Theor. Biol.* **252**:546 – 554.  
doi: <http://dx.doi.org/10.1016/j.jtbi.2007.10.032>.
  - [7] Hofmeyr, J.-H.S. (1995) Metabolic regulation: a control analytic perspective. *J. Bioenerg. Biomembr.* **27**:479 – 489.  
doi: <http://dx.doi.org/10.1007/BF02110188>.
  - [8] Kacser, H., Burns, J.A. and Fell, D.A. (1995) The control of flux: 21 years on. *Biochem. Soc. Trans.* **23**:341 – 366.
-

- 
- [9] Hofmeyr, J.-H.S. and Cornish-Bowden, A. (1997) The reversible Hill equation: how to incorporate cooperative enzymes into metabolic models. *Comp. Appl. Biosci.* **13**:377–385
  - [10] Fell, D.A. and Sauro, H.M. (1985) Metabolic control and its analysis. Additional relationships between elasticities and control coefficients. *Eur. J. Biochem.* **148**:555–561.  
doi: <http://dx.doi.org/10.1111/j.1432-1033.1985.tb08876.x>.
  - [11] Hofmeyr, J.-H.S., Cornish-Bowden, A. and Rohwer, J.M. (1993) Taking enzyme kinetics out of control; putting control into regulation. *Eur. J. Biochem.* **212**:833–837.  
doi: <http://dx.doi.org/10.1111/j.1432-1033.1993.tb17725.x>.
  - [12] Hofmeyr, J.-H.S. and Cornish-Bowden, A. (1996) Co-response analysis: A new experimental strategy for metabolic control analysis. *J. Theor. Biol.* **182**:371–380.  
doi: <http://dx.doi.org/10.1006/jtbi.1996.0176>.
  - [13] Hofmeyr, J.-H.S. and Cornish-Bowden, A. (1991) Quantitative assessment of regulation in metabolic systems. *Eur. J. Biochem.* **200**:223–236.  
doi: <http://dx.doi.org/10.1111/j.1432-1033.1991.tb21071.x>.
  - [14] Chassagnole, C., Fell, D.A., Raÿs, B., Kudla, B. and Mazat, J.-P. (2001) Control of the threonine-synthesis pathway in *Escherichia coli*: a theoretical and experimental approach. *Biochem. J.* **356**:433–444.  
doi: <http://dx.doi.org/10.1042/0264-6021:3560433>.
  - [15] Holzhütter, H.-G. (2004) The principle of flux minimization and its application to estimate stationary fluxes in metabolic networks. *Eur. J. Biochem.* **271**:2905–2922.  
doi: <http://dx.doi.org/10.1111/j.1432-1033.2004.04213.x>.
  - [16] Schuster, S., Kahn, D. and Westerhoff, H.V. (1993) Modular analysis of the control of complex metabolic pathways. *Biophys. Chem.* **48**:1–17.  
doi: [http://dx.doi.org/10.1016/0301-4622\(93\)80037-J](http://dx.doi.org/10.1016/0301-4622(93)80037-J).
  - [17] Brown, G.C., Hafner, R.P. and Brand, M.D. (1990) A 'top-down' approach to the determination of control coefficients in metabolic control theory. *Eur. J. Biochem.* **188**:321–325.  
doi: <http://dx.doi.org/10.1111/j.1432-1033.1990.tb15406.x>.
  - [18] Quant, P.A. (1993) Experimental application of top-down control analysis to metabolic systems. *Trends Biochem. Sci.* **18**:26–30.  
doi: [http://dx.doi.org/10.1016/0968-0004\(93\)90084-Z](http://dx.doi.org/10.1016/0968-0004(93)90084-Z).
-

- [19] Rohwer, J.M., Schuster, S. and Westerhoff, H.V. (1996) How to recognize mono-functional units in a metabolic system. *J. Theor. Biol.* **179**:213 – 228.  
doi: <http://dx.doi.org/10.1006/jtbi.1996.0062>.
- [20] Olivier, B.G., Rohwer, J.M. and Hofmeyr, J.-H.S. (2005) Modelling cellular systems with PySCeS. *Bioinformatics* **21**:560 – 561.  
doi: <http://dx.doi.org/10.1093/bioinformatics/bti046>.
- [21] Hucka, M., Finney, A., Sauro, H.M., Bolouri, H., Doyle, J.C., Kitano, H., Arkin, A.P., Bornstein, B.J., Bray, D., Cornish-Bowden, A., Cuellar, A.A., Dronov, S., Gilles, E.D., Ginkel, M., Gor, V., Goryanin, I.I., Hedley, W.J., Hodgman, T.C., Hofmeyr, J.-H., Hunter, P.J., Juty, N.S., Kasberger, J.L., Kremling, A., Kummer, U., LeNovère, N., Loew, L.M., Lucio, D., Mendes, P., Minch, E., Mjolsness, E.D., Nakayama, Y., Nelson, M.R., Nielsen, P.F., Sakurada, T., Schaff, J.C., Shapiro, B.E., Shimizu, T.S., Spence, H.D., Stelling, J., Takahashi, K., Tomita, M., Wagner, J. and Wang, J. (2003) The systems biology markup language (SBML): a medium for representation and exchange of biochemical network models. *Bioinformatics* **19**:524 – 531.  
doi: <http://dx.doi.org/10.1093/bioinformatics/btg015>.

